Diagrammatic derivation of Bose condensate fractions

Tilo Wettig* and A. D. Jackson
Department of Physics, State University of New York at Stony Brook, Stony Brook, New York 11794-3800
(Received 21 April 1995; revised manuscript received 4 August 1995)

We describe a diagrammatic calculation of the condensate fraction of dense and strongly interacting Bose systems at zero temperature using the framework of parquet theory. Starting from the proper self-energy of parquet theory we perform a major rearrangement of diagrams to ensure proper counting and to express the final result in terms of well-behaved quantities. A number of interesting limiting cases are considered, in particular the hard sphere Bose gas at low densities where analytical results can be obtained. The present formalism is well-suited for extension to finite temperatures, and we consider possible strategies in that direction.

I. INTRODUCTION

The phenomenon of Bose-Einstein condensation (BEC) has long been a subject of great interest and extensive research. Although the original motivation came from the well-known properties of liquid ^{4}He many decades ago, there is presently a renewed interest in BEC in a variety of systems including excitons in Cu_2O,[1] spin-polarized atomic hydrogen,[2] and kaons in dense nuclear matter.[3–5] Also, BEC is believed to play a role in high-T_c superconductors.[6]

Although a well-defined many-body theory exists and is, in principle, capable of a complete description of this phenomenon,[7] it is far too complicated to obtain useful analytical results except in the special cases of weak interaction and low density. The most famous example is a system of hard spheres of radius a at a density ρ. Here, analytical results have been obtained by Lee, Huang, and Yang[8–10] and by Wu[11] who determined the leading terms of a perturbative expansion in the parameter $\sqrt{\rho a^3}$. It is instructive to estimate the useful range of this expansion for the realistic case of liquid ^{4}He for which a is roughly 2 Å. If we require that the second-order correction to the ground state energy be less than 50% of the first-order contribution, the density should be less than 10^{-5} Å^{-3}. This is to be compared with the empirical equilibrium density of liquid ^{4}He which is 0.021 85 Å^{-3}. Given the complexity of the underlying exact many-body theory, it is clear that approximate theories must be formulated to deal with the realistic cases of dense and strongly interacting systems.

Let us first consider the situation at zero temperature. There exists a number of approximate theories which can be roughly divided into variational approaches,[12,13] diagrammatic approaches, and the elegant but numerically demanding Green's function Monte Carlo (GFMC) method[14,15] which yields an essentially exact solution of the many-body Schrödinger equation. The most successful variational theories make use of the so-called hypernetted chain (HNC) approximation[16,17] and can be improved perturbatively using the method of correlated basis functions (CBF).[13,18] The simplest diagrammatic approach which contains all ingredients necessary to ensure that all observable quantities are well behaved (and, thus, provides a suitable starting point for perturbative improvements) is known as parquet theory.[19–21] By making well-defined approximations, it is possible to demonstrate that the underlying physical contents of the HNC approximation and parquet theory are identical.[22] Each of these theories yields remarkably reliable results for quantities such as the ground state energy or the static liquid structure function of dense and strongly interacting Bose systems. While a formalism for HNC calculations of the condensate fraction exists,[23–26] the analogous formalism has not yet been constructed in parquet theory. Such construction is the object of the present paper, and we will draw parallels between the two approaches whenever possible.

Eventually, the goal is to extend the zero-temperature formalism to finite temperatures. For example, one would like to compute the temperature at which the condensate fraction of liquid ^{4}He becomes zero in order to compare with the experimentally observed λ transition at $T=2.17$ K. This problem has not been solved. Initial attempts at finite-temperature calculations have been made in both variational and diagrammatic approaches,[27–30] but reliable calculations of the condensate fraction and the λ point have not yet been achieved. Nonzero temperature also leads to significant complication of the GFMC method which must be replaced by the path integral Monte Carlo (PIMC) method, which requires even greater computational efforts and results in somewhat larger error bars. Although PIMC data hint at a roughly correct value of T_λ,[31] the error bars are too large to draw unambiguous conclusions. At first glance, it would appear that it is simpler to extend approximate diagrammatic theories to finite temperature than variational theories. In principle, diagrammatic theories merely require the replacement of zero-temperature Green's functions by their well-known finite-temperature analogs. While this replacement is numerically challenging, it is conceptually simple. Unfortunately, the problem is not so simple since finite temperature also changes the way in which diagrams should be grouped and (approximately) summed. We shall discuss some possible strategies which might be adopted in this case.

The organization of this paper is as follows. Section II deals with the diagrammatic derivation of the condensate fraction in parquet theory and contains the main results of the paper. A number of interesting limiting cases, including the famous hard sphere Bose gas, will be considered in Sec. III. A discussion of the possible extension of the present

results to finite temperatures is given in Sec. IV, and a variety of conclusions are drawn in Sec. V. Three appendixes are provided for the more technical details of the derivation in Sec. II.

II. DIAGRAMMATIC DERIVATION OF THE CONDENSATE FRACTION

In this section, we construct a diagrammatic description of the condensate fraction n_c within the framework of parquet theory. For a discussion of the necessary techniques and the notation we refer the reader to Refs. 19 and 21. Here, we note only that we treat a homogeneous system of bosons as a system of fermions with an artificial degeneracy ν equal to the number of particles A by taking the simultaneous limits $k_F \to 0$ and $\nu \to \infty$ (k_F is the Fermi momentum).[32]

Before proceeding, we point out that, with well-defined kinematic approximations, the parquet equations reduce exactly to the HNC/0 equations derived in variational theory.[33] Thus, there is a close connection between these two approaches although their starting points might appear to be completely different. We shall see that there is a similar connection in the case of the condensate fraction.

The condensate fraction is that fraction of the particles which occupies the $\mathbf{k}=0$ state. In our fermionic formalism, this corresponds to the particles having momentum less than k_F (since $k_F \to 0$). Explicit counting rules are needed in going from the proper self-energy $\Sigma^\star(\mathbf{k},\omega)$ to n_c in order to ensure that diagrammatic truncations do not introduce counting errors. A major rearrangement of diagrams will be necessary to express n_c in terms of small and well-behaved quantities such as the four-point function Γ and to eliminate all reference to the bare potential V. We will argue on purely diagrammatic grounds and neglect for the moment details of the kinematic approximations necessary for numerical implementation.

The full propagator is

$$G^{\alpha\beta}(\mathbf{k},\omega)=\delta_{\alpha\beta}\left[\frac{\theta(k-k_F)}{\omega-\omega_k-\Sigma^\star(\mathbf{k},\omega)+i\eta}+\frac{\theta(k_F-k)}{\omega-\omega_k-\Sigma^\star(\mathbf{k},\omega)-i\eta}\right], \tag{1}$$

where α and β label the fictitious ''spin'' quantum number of the Fermi system, and η is an infinitesimal positive constant. Units are chosen such that $\omega_k=k^2/2$. The number density of particles in the condensate, $\rho_c=n_c\rho$, can be obtained immediately:

$$\rho_c=-i\nu\int\frac{d^4k}{(2\pi)^4}\theta(k_F-k)G(\mathbf{k},\omega)e^{i\epsilon\omega}=-i\nu\int\frac{d^4k}{(2\pi)^4}\frac{\theta(k_F-k)}{\omega-\omega_k-\Sigma^\star(\mathbf{k},\omega)-i\eta}e^{i\epsilon\omega}. \tag{2}$$

Here, ϵ is an infinitesimal positive constant that ensures convergence of the ω integration. Specifically, it forces us to close the contour of integration in the upper half-plane. Performing the integration over d^3k in the limit $k_F\to 0, \nu\to\infty$, we obtain

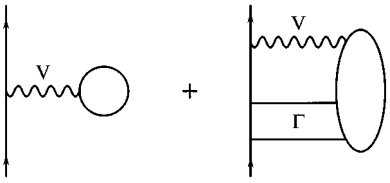

FIG. 1. The proper self-energy, $\Sigma^\star(\mathbf{k},\omega)$, in parquet theory. The incoming and outgoing lines carry four-momentum $(\mathbf{k},\omega)$.

$$n_c=-i\int\frac{d\omega}{2\pi}\frac{1}{\omega-\Sigma^\star(0,\omega)-i\eta}e^{i\epsilon\omega}. \tag{3}$$

In order to perform the ω integration we must determine all zeros of the denominator in the above expression. The explicit form of $\Sigma^\star(0,\omega)$ in approximate parquet theory guarantees that there is one and only one zero at $\omega=\omega_0$ where ω_0 is real and negative. The ω integration is now performed by closing the contour in the upper half-plane. We obtain

$$n_c=\frac{1}{1-\left.\frac{\partial\Sigma^\star(0,\omega)}{\partial\omega}\right|_{\omega_0}}. \tag{4}$$

While it is, in principle, necessary to determine ω_0 exactly, it would be very convenient if one could find an approximate location for this zero. Numerical studies indicate that the value $\omega_0=0$ provides a very good approximation for the exact location. We shall use this approximation in the following so that our basic equation for the condensate fraction becomes

$$n_c=\frac{1}{1-\left.\frac{\partial\Sigma^\star(0,\omega)}{\partial\omega}\right|_{\omega=0}}. \tag{5}$$

Given the explicit diagrammatic form of $\Sigma^\star$ in parquet theory as shown in Fig. 1, we can now proceed to calculate the derivative of $\Sigma^\star(0,\omega)$ with respect to ω at $\omega=0$. The first diagram in Fig. 1 evaluates to $\rho V(k=0)$ and is, therefore, independent of the incoming four-momentum. It does not contribute to the desired derivative. Our attention now focuses entirely on the second diagram in Fig. 1.

Differentiation of this diagram with respect to the fourth component ω of the incoming four-momentum means differentiation of every piece of the diagram that depends on this ω. The only explicit reference to ω is contained in the leftmost particle line. Since approximate parquet theory neglects all self-energy insertions, this and every other explicit particle line is understood to correspond to a free propagator $G^0_{\alpha\beta}(\mathbf{k},\omega)$, obtained from Eq. (1) by setting $\Sigma^\star(\mathbf{k},\omega)$ equal to zero. Its ω derivative is simply

$$\frac{\partial G_0^{\alpha\beta}(\mathbf{k},\omega)}{\partial\omega}=-[G_0^{\alpha\beta}(\mathbf{k},\omega)]^2. \tag{6}$$

From now on, we will label a differentiated particle line in a diagram by an $\times$ on this line. This is equivalent to substituting $-G_0^2$ for G_0 when the diagram is to be evaluated according to the Feynman rules.

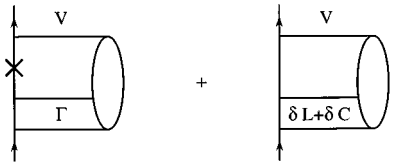

FIG. 2. Diagrams contributing to $\partial\Sigma^{\star}(0,\omega)/\partial\omega|_{\omega=0}$. The incoming and outgoing particle lines carry four-momentum zero.

In addition to the explicit ω dependence of the leftmost particle line there is an implicit ω dependence in Γ in the second diagram of Fig. 1. Recall that $\Gamma = V + L + C$, where L and C are ladder and chain diagrams, respectively. Denoting the ω derivatives (evaluated at $\omega = 0$) of L and C by δL and δC, respectively, we can represent $\partial\Sigma^{\star}(0,\omega)/\partial\omega|_{\omega=0}$ as the sum of the two diagrams in Fig. 2.

The next step is to determine δL and δC. This is (almost) straightforward given the parquet equations for L and C,

$$L = (V+C)G_{\rm pp}(V+C) + (V+C)G_{\rm pp}L, \tag{7a}$$

$$C = (V+L)G_{\rm ph}(V+L) + (V+L)G_{\rm ph}C. \tag{7b}$$

Here, $G_{\rm pp}$ and $G_{\rm ph}$ are particle-particle (pp) and particle-hole (ph) propagators, respectively. The bare potential V is local and, hence, independent of ω. Applying the chain rule should then yield expressions for δL and δC. However, there is one subtlety. In any given diagram, the only reference to the *external* ω lies in the leftmost particle line. It is only at this line where differentiation with respect to the external ω occurs. This places no restrictions on the number of particle-particle propagators involved. However, as soon as some momentum ''branches'' to the right through a particle-hole propagator, there will be no further reference to the external ω in the rest of the chain following this particle-hole propagator. With this observation, we are able to formulate equations for δL and δC:

$$\delta L = (V+C)\,\delta G_{\rm pp}\Gamma + \delta C G_{\rm pp}\Gamma + (V+C)G_{\rm pp}(\delta L + \delta C), \tag{8a}$$

$$\delta C = \delta L G_{\rm ph}\Gamma. \tag{8b}$$

Here, $\delta G_{\rm pp}$ denotes a particle-particle propagator whose left single particle line is differentiated with respect to the external ω (i.e., this particle line is marked by an $\times$). The fact that a particle-hole propagator eliminates all reference to the external ω is reflected in the equation for δC.

Using Eq. (7a), Eq. (8a) can be brought into a more convenient form which eliminates all reference to the bare potential (which is generally ill behaved) in favor of Γ (which is the smallest quantity available and well behaved). These manipulations are performed in Appendix A. We obtain

$$\delta L + \delta C = \Gamma\,\delta G_{\rm pp}\Gamma + (1+\Gamma G_{\rm pp})\,\delta C(1+G_{\rm pp}\Gamma), \tag{9a}$$

$$\delta C = \delta L G_{\rm ph}\Gamma. \tag{9b}$$

The two diagrams in Fig. 2 which determine $\partial\Sigma^{\star}(0,\omega)/\partial\omega|_{\omega=0}$ still contain a factor of the bare potential. In order to exploit the cancellations inherent in Γ as fully as possible, we would like to rearrange these diagrams so that bare potential lines do not appear. Also, we would like the resulting diagrams to be top-bottom symmetric. This is not merely an aesthetic desire. It also helps guarantee that the symmetries of the underlying physical processes will be respected in our approximate treatment.

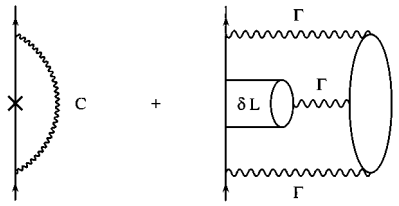

FIG. 3. A better-behaved form for $\partial\Sigma^{\star}(0,\omega)/\partial\omega|_{\omega=0}$. Again, the incoming and outgoing particle lines carry four-momentum zero.

The necessary rearrangements can be made using Eqs. (7a) and (9). They are, however, neither straightforward nor simple and are therefore described in Appendix B. The final result can again be expressed in terms of two diagrams which are shown in Fig. 3.

Let us focus our attention on the second diagram in Fig. 3. Its leading contribution to $\partial\Sigma^{\star}(0,\omega)/\partial\omega|_{\omega=0}$ is of fifth order in the potential. For weak potentials and/or low density, this contribution will be negligible compared with the contribution of the first diagram. Also, the diagram contains three factors of Γ. As mentioned before, Γ is the smallest quantity available. It reflects maximal cancellations between short-range repulsion and long-range attraction. Thus, even if the potential is not weak or the density is not low, we expect this diagram to make a small contribution compared with the contribution from the first diagram. This expectation is supported by numerical studies. Our second approximation, therefore, is to neglect this diagram altogether. This approximation results in a considerable simplification of subsequent calculations.

We have arrived at a fairly simple form for the condensate fraction. However, the appearance of a marked propagator in the first diagram of Fig. 3 suggests that it may be necessary to take a closer look at diagrams which have been neglected along the way. Our starting point for the present considerations was Fig. 1 which is a result of approximate parquet theory. This approximation neglects all vertex corrections and all self-energy insertions in any given diagram; the main reason for this neglect (apart from a desire for simplicity) is the fact that first-order vertex corrections and self-energy insertions are strictly absent in Bose systems. Inclusion of these effects would have consequences of two different types

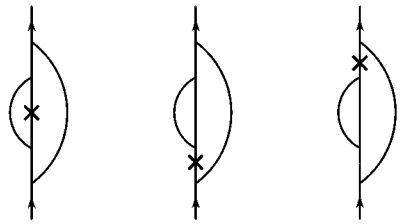

FIG. 4. The second and the third diagrams can still be interpreted as containing self-energy insertions. This is no longer possible for the first diagram due to the marked propagator.

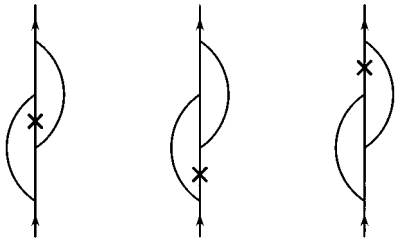

FIG. 5. The second and the third diagrams can still be interpreted as containing vertex corrections. This is no longer possible for the first diagram due to the marked propagator.

for the determination of the condensate fraction. The ω differentiation (and the marked propagator) can occur at a place accessible to approximate parquet theory as in the second and third diagrams shown in Figs. 4 and 5. Propagator and vertex corrections remain such after the differentiation. These effects can be evaluated by constructing n_c in the bare theory (as above) and ''merely'' replacing all bare propagators and vertices by the corresponding dressed quantities. This can result in numerical changes but not in structural changes. However, the ω differentiation of a fully dressed diagram can also occur at a location not accessible to approximate parquet theory as in the first diagrams shown in Figs. 4 and 5. These are structurally new contributions to n_c which materially alter the counting of diagrams contributing to the condensate fraction. Since our primary concern here is with the counting of diagrams and not with their numerical evaluation, we will continue to neglect all diagrams which contain explicit vertex corrections and/or self-energy insertions (e.g., the second and third diagrams in Figs. 4 and 5). We will, however, explicitly reinstate structurally new diagrams such as the first diagrams in Figs. 4 and 5. Many more new diagrams will be generated in higher orders in C. Specifically, in order n, there will be $n!$ diagrams contributing to $\partial\Sigma^{\star}(0,\omega)/\partial\omega|_{\omega=0}$. This follows from the fact that there are $n!$ distinct ways to mark the leftmost propagator in nth order. (See Figs. 12 and 13, below, in this respect.)

Fortunately, one additional (kinematic) approximation renders explicit evaluation of these diagrams unnecessary. We demonstrate in Appendix C that all additional diagrams can be included by exponentiating the first diagram in Fig. 3. The approximation involved can be seen to be controlled and reliable. Our final result for the condensate fraction is simply

$$n_c = \exp(D), \tag{10}$$

where D is the value of the first diagram in Fig. 3 as evaluated according to the Feynman rules.

Note that Eq. (10) always predicts a nonzero condensate fraction at $T=0$. This fact provides an initial signal that the approximation leading to Eq. (10) may not be valid for nonzero temperature since we expect that all systems of interest will have a finite transition temperature. While this could arise through singularities in D, it seems more likely that the approximations leading to exponentiation break down. We shall return to this question in Sec. IV. It is also interesting to note that Eq. (10) has the same structure as the HNC result for the condensate fraction.[24] Unfortunately, a detailed diagrammatic interpretation of the HNC exponent requires a fairly precise discussion of how a special subset of ladder diagrams is to be incorporated in the evaluation of D. Ladder diagrams in this subset contain one and only one pp propagator where both intermediate particles are in the condensate simultaneously. The contribution of these diagrams to, e.g., the binding energy per particle or the static structure function is numerically small compared to the contribution of all ladder diagrams so that little attention has been paid to this point previously. Unfortunately, this is not the case for the condensate fraction so that this question should be addressed with greater care. Here, we are concerned primarily with the structure of the diagrammatic derivation. Details associated with the correct counting of these special diagrams will be considered in a separate publication.

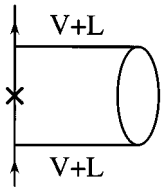

FIG. 6. In the limiting case of pure ladders, the condensate fraction is determined by this diagram.

III. LIMITING CASES

In this section, we consider three particularly interesting limiting cases of the results of the preceding section. These will be (i) the pure ladder sum, (ii) the pure chain [or random phase approximation (RPA)] sum, and (iii) the hard sphere system.

A. Pure ladders

The pure ladder limit is obtained by setting the chains equal to zero. Looking at Fig. 3, there appears to be nothing left to calculate. We must recall, however, that Fig. 3 was the result of a considerable rearrangement of diagrams. To obtain the correct ladder limit, we look back at the proper self-energy shown in Fig. 1. It is now given by the sum of all pure ladder diagrams closed off with a bare propagator. In each diagram of order n in V, there are $n-1$ distinct ways to mark the leftmost particle line. Correct counting rules allow for the inclusion of the full ladder sum before and after the marked propagator. Thus, the condensate fraction is determined by the diagram in Fig. 6. Explicit evaluation of this diagram yields

$$D_L = -i\int \frac{d^4k}{(2\pi)^4}\,\theta(k-k_F)G_0^2(\mathbf{k},\omega)\,\pi_0(\mathbf{k},\omega)(V_k+L_k)^2$$
$$= -\frac{\rho}{4}\int \frac{d^3k}{(2\pi)^3}\,\frac{(V_k+L_k)^2}{\omega_k^2}. \tag{11}$$

Here, $\pi_0(\mathbf{k},\omega)$ denotes a particle-hole propagator which is given as

$$\pi_0(\mathbf{k},\omega) = -i\nu \int \frac{d^4p}{(2\pi)^4} G_0(k+p) G_0(p)$$

$$= \frac{2\rho\omega_k}{(\omega-\omega_k+i\eta)(\omega+\omega_k-i\eta)}. \tag{12}$$

L is obtained from the ladder equation, Eq. (7a), with the replacement of C by zero. After performing the integration over the fourth component of the intermediate momentum we obtain

$$L(k) = \int \frac{d^3p}{(2\pi)^3} V(|\mathbf{p}+\mathbf{k}|) \frac{1}{(-2\omega_p)} [V(p)+L(p)]. \tag{13}$$

Barring special dynamical circumstances, the quantity $V_k + L_k$ will be nonzero at $k=0$. Hence, the integrand of Eq. (11) behaves like $1/k^2$ in the small-k limit, and the integral is divergent. We obtain an unphysical result. This is an indication of the absolute necessity of summing the chain diagrams (or RPA) for Bose systems.[21]

B. Pure chains or the RPA limit

The RPA limit is obtained by neglecting the ladders in the defining equation for the chains, Eq. (7b). The calculation for this case is performed in Appendix III. Indeed, Eq. (34) yields

$$D_{\mathrm{RPA}} = -\frac{1}{\rho} \int \frac{d^3k}{(2\pi)^3} \frac{(\epsilon_k-\omega_k)^2}{4\epsilon_k\omega_k}, \tag{14}$$

where $\epsilon_k^2 = \omega_k^2 + 2\rho\omega_k V(k)$. The integrand is now proportional to k in the small-k limit, so that the integral is finite. This result of Eq. (14) is precisely the same as the uniform limit of the HNC condensate fraction.[34]

C. Hard sphere limit

The limit of a dilute gas of hard spheres is especially interesting since analytical results have been obtained using a variety of methods.[8–10] In Ref. 21 we showed that parquet theory correctly reproduces the binding energy obtained in Ref. 9. The aim of this section is to demonstrate that the condensate fraction obtained in Ref. 10 is also reproduced by our formalism.

We briefly summarize the arguments used in Ref. 21 to treat the hard sphere system. We consider a hard-core potential of range a; i.e., the potential is simply

$$V(r) = \begin{cases} +\infty & \text{for} \quad r<a, \\ 0 & \text{for} \quad r>a. \end{cases} \tag{15}$$

We construct the ladder sum using the bare potential in analogy with Eq. (13). This ladder sum is then used to drive the chain equation. This procedure is sensible if the density is relatively low or the range of the core is relatively small (i.e., if $\rho a^3 \ll 1$).

Equation (13) can be solved analytically for a potential of finite height $V_0 = \kappa^2$ and range a.[35] We obtain

$$V(k) + \tilde{L}(k) = 4\pi a \left[\frac{\sin ka}{ka} - \cos ka \frac{\tanh \kappa a}{\kappa a} \right] \frac{\kappa^2}{k^2+\kappa^2}, \tag{16}$$

where $\tilde{L}$ denotes the zero-density approximation to the correct ladder sum, L. The hard-core limit of Eq. (16), $\kappa^2 \to \infty$, is simply

$$V(k) + \tilde{L}(k) = 4\pi a \frac{\sin ka}{ka}. \tag{17}$$

The effective potential $V_{\mathrm{eff}} = V + \tilde{L}$ represents an appropriate driving term for the chains. Naively, the condensate fraction can then be obtained from Eq. (14) through the substitution of V by V_{eff} in ϵ_k. In the determination of the binding energy, a counting problem arose in connection with the second-order contribution of V_{eff} to E/A.[21] This is not the case for the condensate fraction where there are no such counting problems due to the presence of the marked propagator on the leftmost line. Hence, the naive expectation is correct.

It remains to compute the integral in Eq. (14). We now have an explicit expression for ϵ_k, $\epsilon_k^2 = \omega_k^2 + 8\pi\rho a \omega_k \sin ka/ka$. Given the structure of the integrand, it is clear that the leading contribution in the present limit comes from the region of small k. There, it is legitimate to approximate $V(k) + \tilde{L}$ by $4\pi a$. This approximation enables us to perform the integration analytically. Specifically,

$$D_{\mathrm{HS}} = -\frac{1}{\rho} \int \frac{d^3k}{(2\pi)^3} \frac{(\sqrt{\omega_k^2 + 8\pi\rho a\omega_k} - \omega_k)^2}{4\omega_k \sqrt{\omega_k^2 + 8\pi\rho a\omega_k}}$$

$$= -4 \left(\frac{\rho a^3}{\pi} \right)^{1/2} \int_0^\infty dz \frac{(\sqrt{1+z}-1)^2}{z^{5/2}\sqrt{1+z}}$$

$$= -\frac{8}{3} \left(\frac{\rho a^3}{\pi} \right)^{1/2}, \tag{18}$$

where HS stands for hard spheres. In the present limit, $\exp(D) \approx 1 + D$ so that

$$n_c^{\mathrm{HS}} = 1 - \frac{8}{3} \left(\frac{\rho a^3}{\pi} \right)^{1/2}. \tag{19}$$

This is precisely the result found in Ref. 10.

IV. TOWARDS FINITE TEMPERATURES

Ultimately, one would like to construct a reliable approximate many-body theory for the finite-temperature case. As indicated in the Introduction, several important steps in this direction have been made in both the variational and the diagrammatic formalisms. Variational theories are more advanced at present, and considerable work has been done both below[27,28] and above[29] the λ point. To date, parquet theory has only been extended to temperatures below the λ point,[30] and the close connection between the two approaches persists at finite temperatures. Thus, the substantial analogies between variational formalisms and parquet theory make the former very useful to guide the development of the latter. However, a reliable calculation of, e.g., the λ point of liquid

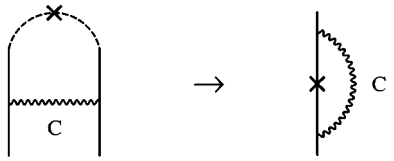

FIG. 7. Closing off the top end points of the chain contribution to Γ with a differentiated propagator yields the first diagram in Fig. 3.

FIG. 8. Closing off the top end points of the second-order ladder diagrams (in C) with a differentiated propagator yields the two diagrams in Fig. 12. Note that we must include the exchange diagram on the right.

[4]He has not been achieved yet in approximate theories, although data from PIMC calculations are available.[31] Hence, further development of approximate theories seems very desirable.

While it is not our aim to provide a detailed discussion of the condensate problem at finite temperatures, several observations about this problem may be useful. At first sight, the extension to $T\neq 0$ seems relatively straightforward in the present formalism. Much of the work of summing diagrams has already been done, and the extension should largely be a matter of replacing zero-temperature Green's functions by their finite-temperature analogs. However, a number of problems and subtleties arise in this extension, and it is the purpose of this section to discuss these in some detail.

One formalism convenient for the treatment of condensed Bose systems at finite temperatures has been developed by Lee[36] in the context of the canonical ensemble. This formalism is likely to be useful for the extension of parquet theory to $T\neq 0$. In Lee's approach, the free propagator is given by

$$G_0(\mathbf{k},\omega_n)=\frac{1}{i\omega_n-\omega_k+\mu_0}, \tag{20}$$

where the ω_n are discrete Matsubara frequencies given by $\omega_n=2\pi n/\beta$ with $\beta=1/k_BT$ (k_B is the Boltzmann constant). The quantity μ_0 is the chemical potential of the noninteracting Bose system at temperature T. Of course, finite-temperature calculations present various technical complications. Instead of performing the relatively simple integrations over ω appropriate for zero temperature, it is necessary to sum over the discrete Matsubara frequencies. While these sums can be done analytically in certain simple cases, results typically depend on the remaining (external) Matsubara frequencies in a complicated way, and further computation is severely hindered. Thus, additional approximations will be called for.[30] Also, an additional counting rule in Lee's formalism leads to certain subtleties in the treatment of condensate propagators. Such problems are largely technical in nature, and we prefer to focus on diagrammatic aspects of the problem.

The tacit (diagrammatic) assumption is that those diagrams which provide the most important contributions to the zero-temperature problem will also be of primary importance for $T\neq 0$. Unfortunately, this assumption is not entirely correct. Many classes of diagrams have been excluded from the parquet formalism because they are strictly zero at $T=0$. Examples include exchange diagrams and vertex corrections involving local potentials. Such diagrams no longer vanish when $T\neq 0$. Indeed, certain classes of these diagrams can be shown to be essential for the cancellation of explicit divergences, and their contributions must be included with care. In particular, it is not obvious that the exponentiation of diagrams, Eq. (10), remains valid for $T\neq 0$. (It is difficult to reconcile exponentiation with a vanishing condensate fraction at the transition temperature.) This exponentiation was obtained by reinstating important diagrams (vertex corrections and self-energy insertions) previously neglected and by demonstrating that their inclusion could be approximated by exponentiating the basic diagram (i.e., the first diagram in Fig. 3).

In general, the four-point function follows from functional differentiation of the proper self-energy with respect to the propagator so that a single diagrammatic contribution to $\Sigma^\star$ leads to many diagrams in Γ. Unfortunately, it is not possible to construct any approximate many-body theory for Γ which maintains complete consistency with $\Sigma^\star$.[37] As a consequence, general rules for proceeding from Γ to $\Sigma^\star$ are not applicable in any approximate theory. Explicit counting rules must be constructed, and their construction is usually not unique. In principle, all algorithms leading to the same set of diagrams are equally valid. In practice, approximations must be made, and different routes will suggest different approximation schemes. Thus, we would like to suggest an equivalent way to recover those ''additional'' diagrams incorporated by exponentiation. This alternate approach is valid at $T=0$ and is likely to be more fruitful when $T\neq 0$ since it provides for the cancellation of new explicit divergences in a natural way.

The basic diagram can also be obtained by the following process: Take the contribution of the chains to the four-point function and close the end points at the top with a marked propagator. This process is depicted in Fig. 7. Similarly, the two diagrams in Fig. 12, below, can be obtained by closing ladder diagrams of second order in the chains in the same way. Figure 8 illustrates this process. One of these ladder diagrams is an exchange diagram. In exactly the same way, all diagrams of higher order in C can be obtained by closing higher-order ladder diagrams. These ladder diagrams must include all possible exchange contributions. In nth order,

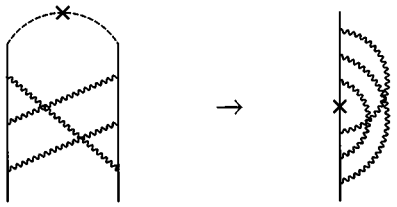

FIG. 9. Closing off the top end points of this third-order ladder diagram (in C) with a differentiated propagator yields the fifth diagram in Fig. 13.

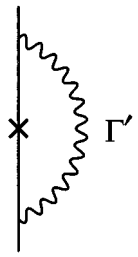

FIG. 10. An alternative diagrammatic representation of the condensate fraction. As described in the text, this diagram includes all the diagrams that had been included through the exponentiation of Eq. (10) at $T=0$. Γ' is the sum of the bare potential V, the ladders including all exchange diagrams L', and the chains C.

there are $n!$ such diagrams corresponding to the $n!$ distinct possibilities of attaching potential (i.e., chain) lines to the line on the right hand side of the ladder diagram. As an example, Fig. 9 demonstrates how the fifth diagram in Fig. 13, below, is obtained in this scheme.

It is clear that this procedure generates all the diagrams previously included through the exponentiation in Eq. (10). Note, however, that it is necessary to retain all possible exchange contributions to the ladder diagrams. All of these exchange contributions are strictly zero at $T=0$ when local potentials are used as rungs. This was the reason for their neglect in the evaluation of the ladders at zero temperature. However, nonlocal rungs (such as ω-dependent chains) yield nonzero exchange diagrams even at $T=0$. Their inclusion was accomplished through the exponentiation in Eq. (10). At finite temperatures, even local rungs give rise to nonzero exchange diagrams. On the one hand, this indicates the need for greater care in the summation of ladder diagrams. On the other hand, it may provide a convenient way to include the ''additional'' diagrams in question without exponentiation.

The contribution of the bare potential to Γ will also make a nonzero contribution to the condensate fraction at finite temperature when closed with a marked propagator in the manner described above. Thus, the basic diagram which yields the condensate fraction at $T\neq 0$ is just the full four-point function, $\Gamma'=V+L'+C$, closed off with a marked propagator. Here, L' denotes the ladder sum including all possible exchange diagrams. See Fig. 10 in this regard. There is no longer any need for exponentiation.

The foregoing discussion has assumed but not specified the existence of a ''marked propagator'' at finite temperatures. At $T=0$, this object arose from a differentiation with respect to the fourth component of the four-momentum which was equivalent to substituting $-G_0^2$ for G_0 in the evaluation of the resulting Feynman diagram. At $T\neq 0$, we must deal with discrete Matsubara frequencies with respect to which we cannot differentiate. However, we can again obtain the result $-G_0^2$ for the marked propagator if we differentiate with respect to the chemical potential which appears in the denominator of the propagator. While there are arguments in support of this procedure, we do not regard this issue as settled.

There are two general problems which remain. The first is how to unify the theories at zero and finite temperature so that the $T\rightarrow 0$ limit of the finite-temperature result will yield the zero-temperature result. The kinematic approximations adopted at $T=0$ (as described in Appendix C) are markedly different from those which would be required in the method described above, so that there is no guarantee that the $T=0$ results would be the same. The second problem is the correct incorporation of the RPA sum in the exchange diagrams. As we have demonstrated in the text, respecting the RPA limit is vital for convergence properties. Clearly, an exact treatment is out of the question due to the technical difficulties associated with the infinite sums over Matsubara frequencies. We suspect that a judicious approximate treatment of the ω dependence may provide a solution not only to the second but also to the first problem.

A better understanding of the finite-temperature properties of condensed Bose systems is highly desirable. Of course, there is still a great amount of work to be done, but efforts along the lines suggested here seem very much worthwhile.

V. CONCLUSIONS

We have derived an interpretation of the condensate fraction of Bose systems at $T=0$ in terms of diagrams of the parquet class. A major rearrangement of diagrams was performed in order to obtain a result which reflects the symmetries of the underlying physical processes and to express this result in terms of small and well-behaved quantities. Important diagrams previously neglected in parquet theory were reinstated simply with the aid of one judicious kinematic approximation. We considered a number of limiting cases and showed that our results can reproduce the uniform limit of the HNC condensate fraction and the perturbative result for the condensate fraction of the hard sphere system.

Two questions remain open. The first is how properly to extend our formalism to finite temperatures. We have discussed this problem in the preceding section and suggested some ideas in this direction. The second question is that of the correct inclusion of the subset of ladder diagrams mentioned at the end of Sec. II and of the construction of reliable kinematic approximations to produce actual numbers for actual physical systems (such as liquid ^{4}He). We will address this problem in a separate publication.

ACKNOWLEDGMENTS

We would like to thank A. Lande for stimulating discussions. This work was partially supported by the U.S. Department of Energy under Grant No. DE-FG02-88ER 40388.

APPENDIX A: SIMPLIFYING δL

We rewrite Eq. (8a) as

$$[1-(V+C)G_{\rm pp}]\delta L=(V+C)\,\delta G_{\rm pp}\Gamma+(V+C)G_{\rm pp}\delta C + \delta C G_{\rm pp}\Gamma. \tag{A1}$$

Formal solution of this equation for δL requires the inverse operator $[1-(V+C)G_{\rm pp}]^{-1}$. From our equation for Γ,

$$\Gamma=V+C+L=(V+C)+(V+C)G_{\rm pp}\Gamma, \tag{A2}$$

we see that

$$[1-(V+C)G_{\rm pp}]^{-1}(V+C)=\Gamma. \tag{A3}$$

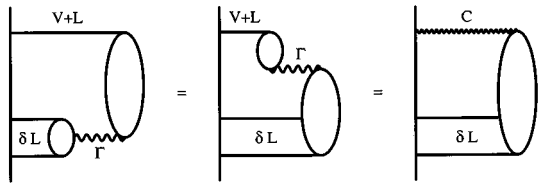

FIG. 11. Three different representations of the same diagram.

Substitution of Eq. (23) into Eq. (21) yields

$$\delta L=\Gamma\,\delta G_{\rm pp}\Gamma+\Gamma G_{\rm pp}\delta C +[1-(V+C)G_{\rm pp}]^{-1}\delta C G_{\rm pp}\Gamma. \tag{A4}$$

For the last term in this equation it is convenient to write the inverse operator in a different form. We multiply Eq. (A2) by $G_{\rm pp}$ on the right and add unity on both sides to obtain

$$\begin{aligned}1&=1+\Gamma G_{\rm pp}-(V+C)G_{\rm pp}-(V+C)G_{\rm pp}\Gamma G_{\rm pp}\\&=[1-(V+C)G_{\rm pp}][1+\Gamma G_{\rm pp}].\end{aligned} \tag{A5}$$

This immediately yields

$$[1-(V+C)G_{\rm pp}]^{-1}=1+\Gamma G_{\rm pp}. \tag{A6}$$

Substituting this form of the inverse operator into Eq. (A4), we obtain

$$\delta L=\Gamma\,\delta G_{\rm pp}\Gamma+\Gamma G_{\rm pp}\delta C+\delta C G_{\rm pp}\Gamma+\Gamma G_{\rm pp}\delta C G_{\rm pp}\Gamma, \tag{A7}$$

which is seen to be identical with Eq. (9a).

APPENDIX B: REARRANGING DIAGRAMS

We think of the second diagram for the proper self-energy in Fig. 1 as a ladder diagram, $\bar{L}=VG_{\rm pp}\Gamma$, closed with a bare propagator, G_0. The corresponding ladder diagrams which, when closed with a bare propagator, lead to the diagrams in Fig. 2 are given as

$$\delta\bar{L}=V\delta G_{\rm pp}\Gamma+VG_{\rm pp}(\delta L+\delta C). \tag{B1}$$

Using Eq. (9), we rewrite this equation as

$$\begin{aligned}\delta\bar{L}&=V\delta G_{\rm pp}\Gamma+VG_{\rm pp}[\Gamma\,\delta G_{\rm pp}\Gamma+(1+\Gamma G_{\rm pp})\,\delta C(1+G_{\rm pp}\Gamma)]\\&=[V+VG_{\rm pp}\Gamma][\,\delta G_{\rm pp}\Gamma+G_{\rm pp}\delta C(1+G_{\rm pp}\Gamma)].\end{aligned} \tag{B2}$$

Since $L=(V+C)G_{\rm pp}\Gamma$, we can replace $V+VG_{\rm pp}\Gamma$ by $V+L-CG_{\rm pp}\Gamma$ in Eq. (B2):

$$\begin{aligned}\delta\bar{L}=&(V+L)\,\delta G_{\rm pp}\Gamma-CG_{\rm pp}\Gamma\,\delta G_{\rm pp}\Gamma+(V+L)G_{\rm pp}\delta C\\&+(V+L)G_{\rm pp}\delta C G_{\rm pp}\Gamma-CG_{\rm pp}\Gamma G_{\rm pp}\delta C\\&-CG_{\rm pp}\Gamma G_{\rm pp}\delta C G_{\rm pp}\Gamma.\end{aligned} \tag{B3}$$

We now use Eq. (9b) to rewrite the third term in Eq. (B3) as $(V+L)G_{\rm pp}(\delta L G_{\rm ph}\Gamma)$. The effect of closing off this diagram with a bare Green's function is equivalent to closing off the diagram $[(V+L)G_{\rm ph}\Gamma]G_{\rm pp}\delta L=CG_{\rm pp}\delta L$ with a bare Green's function. This process is depicted in Fig. 11.

Ultimately, we are interested only in diagrams which contribute to the condensate fraction. We define a new quantity, $\delta\tilde{L}$, by replacing the third term in Eq. (B3) by $CG_{\rm pp}\delta L$. Closing off $\delta\tilde{L}$ with a bare propagator yields exactly the same set of diagrams that would be obtained by closing off $\delta\bar{L}$ with a bare propagator. Using Eq. (A7), we obtain

$$\begin{aligned}\delta\tilde{L}=&(V+L)\,\delta G_{\rm pp}\Gamma-CG_{\rm pp}\Gamma\,\delta G_{\rm pp}\Gamma\\&+CG_{\rm pp}[\Gamma\,\delta G_{\rm pp}\Gamma+\Gamma G_{\rm pp}\delta C+\delta C G_{\rm pp}\Gamma\\&+\Gamma G_{\rm pp}\delta C G_{\rm pp}\Gamma]\\&+(V+L)G_{\rm pp}\delta C G_{\rm pp}\Gamma-CG_{\rm pp}\Gamma G_{\rm pp}\delta C\\&-CG_{\rm pp}\Gamma G_{\rm pp}\delta C G_{\rm pp}\Gamma.\end{aligned} \tag{B4}$$

A number of desirable cancellations lead to

$$\begin{aligned}\delta\tilde{L}&=(V+L)\,\delta G_{\rm pp}\Gamma+(V+L)G_{\rm pp}\delta C G_{\rm pp}\Gamma+CG_{\rm pp}\delta C G_{\rm pp}\Gamma\\&=(V+L)\,\delta G_{\rm pp}\Gamma+\Gamma G_{\rm pp}(\delta L G_{\rm ph}\Gamma)G_{\rm pp}\Gamma.\end{aligned} \tag{B5}$$

Closing off $\delta\tilde{L}$ in this form leads precisely to the two diagrams in Fig. 3. In the first diagram, we have made use of the chain equation $C=(V+L)G_{\rm ph}\Gamma$.

APPENDIX C: EXPONENTIATING DIAGRAMS

We wish to construct a simple but reliable kinematic approximation which facilitates evaluation of all the diagrams contributing to $\partial\Sigma^\star(0,\omega)/\partial\omega|_{\omega=0}$. Using Eqs. (7b) (with $G_{\rm ph}=\pi_0$) and (12), we first construct $C(\mathbf{k},\omega)$. We obtain

$$C(\mathbf{k},\omega)=\frac{(\epsilon_k^2-\omega_k^2)^2}{2\rho\omega_k(\omega-\epsilon_k+i\eta)(\omega+\epsilon_k-i\eta)}, \tag{C1}$$

where $\epsilon_k^2=\omega_k^2+2\rho\omega_k\bar{V}_k$. (Here, $\bar{V}_k$ stands for a generic particle-hole irreducible potential driving the chains.) We de-

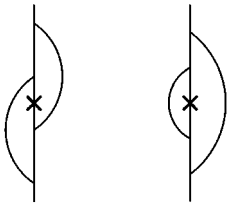

FIG. 12. Diagrams contributing to $\partial\Sigma^\star(0,\omega)/\partial\omega|_{\omega=0}$ in second order in C.

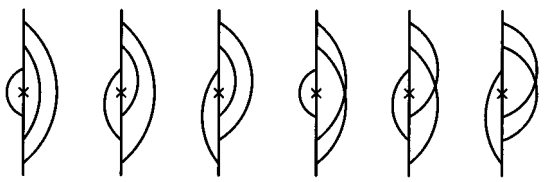

FIG. 13. Diagrams contributing to $\partial\Sigma^\star(0,\omega)/\partial\omega|_{\omega=0}$ in third order in C.

note the value of the first diagram in Fig. 3 by x. Given the explicit form of $C(\mathbf{k},\omega)$, x evaluates to

$$x=-i\int\frac{d^4k}{(2\pi)^4}\frac{(\epsilon_k^2-\omega_k^2)^2}{(\omega-\omega_k+i\eta)^2 2\rho\omega_k}\times\frac{1}{(\omega-\epsilon_k+i\eta)(\omega+\epsilon_k-i\eta)}=-\frac{1}{\rho}\int\frac{d^3k}{(2\pi)^3}\frac{(\epsilon_k-\omega_k)^2}{4\omega_k\epsilon_k}. \tag{C2}$$

We now turn to the evaluation of higher-order diagrams in C. As we have argued in Sec. II, there are $n!$ diagrams in nth order. The second- and third-order contributions to $\partial\Sigma^\star(0,\omega)/\partial\omega|_{\omega=0}$ are illustrated in Figs. 12 and 13, respectively. We will denote the contribution of the ith diagram in nth order by x_{ni}. Hence, i runs from 1 to $n!$.

After the usual ω integrations have been performed analytically, the first diagram in Fig. 12 evaluates to

$$x_{21}=-\frac{1}{\rho^2}\int\frac{d^3k}{(2\pi)^3}\frac{d^3p}{(2\pi)^3}\frac{(\epsilon_k-\omega_k)^2}{4\omega_k\epsilon_k}\frac{(\epsilon_p-\omega_p)^2}{4\omega_p\epsilon_p}\times\frac{(\epsilon_p+\omega_p)^2}{(\epsilon_k+\epsilon_p+\omega_{k+p})^2}. \tag{C3}$$

Equation (C3) has intentionally been written in a suggestive fashion. If the denominator of the last term on the right hand side were independent of k, the two integrals would factor into two independent integrals over d^3k and d^3p. A natural approximation, therefore, is to first replace ω_{k+p} by $\omega_k+\omega_p$ (an ''angle average'' approximation) and then replace k by p in this denominator. The result now becomes extremely simple:

$$x_{21}=-\frac{x^2}{(2!)^2}.$$

Evaluation of the second diagram in Fig. 12 yields

$$x_{22}=-\frac{1}{\rho^2}\int\frac{d^3k}{(2\pi)^3}\frac{d^3p}{(2\pi)^3}\frac{(\epsilon_k-\omega_k)^2}{4\omega_k\epsilon_k}\frac{(\epsilon_p-\omega_p)^2}{4\omega_p\epsilon_p}\times\frac{(\epsilon_k+\omega_k)(\epsilon_p+\omega_p)}{(\epsilon_k+\epsilon_p+\omega_{k+p})^2}. \tag{C4}$$

Again, we replace ω_{k+p} by $\omega_k+\omega_p$ in the last denominator on the right hand side of Eq. (C4). To maintain symmetry between k and p, we once replace k by p and once p by k in one of the two factors in this denominator, respectively. This leads to

$$x_{22}=-\frac{x^2}{(2!)^2}.$$

The pattern has become obvious by now. Equivalent kinematic approximations can be constructed in exactly the same way in higher orders. Each diagram in order n evaluates to $-(-x)^n/(n!)^2$. There are $n!$ diagrams in this order, yielding a total contribution of $-(-x)^n/n!$ to $\partial\Sigma^\star(0,\omega)/\partial\omega|_{\omega=0}$. Thus,

$$\left.\frac{\partial\Sigma^\star(0,\omega)}{\partial\omega}\right|_{\omega=0}=-\sum_{n=1}^{\infty}\frac{(-x)^n}{n!}=1-\exp(-x). \tag{C5}$$

Substitution of Eq. (C5) into Eq. (5) yields Eq. (10) immediately.

The form of the above kinematic approximations was guided by a desire to make calculations tractable and to maintain symmetry between the kinematic variables appearing in the various integrals. They are, however, also numerically reliably. The error introduced by these approximations is not substantial. The dominant contribution to a given integral (say, over d^3k) comes from the region of small argument given the structure of the integrand. There, ϵ_k dominates ω_k so that the replacement of ω_{k+p} by $\omega_k+\omega_p$ has virtually no effect on the value of the integrand. Furthermore, the replacement of k by p does not alter the threshold behavior of the integrand. This leads us to believe that the overall error made is small. We have verified this assumption by numerical studies using interactions and densities appropriate of liquid ^{4}He.

*Present address: Max-Planck-Institut für Kernphysik, 69117 Heidelberg, Germany.

[1] J.-L. Lin and J. P. Wolfe, Phys. Rev. Lett. **71**, 1223 (1993).
[2] Y. Kagan and G. V. Shlyapnikov, Phys. Lett. A **130**, 483 (1988).
[3] D. B. Kaplan and A. E. Nelson, Phys. Lett. B **175**, 57 (1986).
[4] A. E. Nelson and D. B. Kaplan, Phys. Lett. B **192**, 193 (1987).
[5] G. E. Brown, K. Kubodera, and M. Rho, Phys. Lett. B **192**, 273 (1987).
[6] J. Ranninger, in *Bose-Einstein Condensation*, Proceedings of the First International Workshop on Bose-Einstein Condensation, 1993, edited by A. Griffin, D. Snoke, and S. Stringari (Cambridge University Press, Cambridge, 1995).
[7] A. L. Fetter and J. D. Walecka, *Quantum Theory of Many-Particle Systems* (McGraw-Hill, New York, 1971).
[8] K. Huang and C. N. Yang, Phys. Rev. **105**, 767 (1957).
[9] T. D. Lee, K. Huang, and C. N. Yang, Phys. Rev. **105**, 1119 (1957).
[10] T. D. Lee, K. Huang, and C. N. Yang, Phys. Rev. **106**, 1135 (1957).
[11] T. T. Wu, Phys. Rev. **115**, 1390 (1959).
[12] W. L. McMillan, Phys. Rev. **138**, A442 (1965).
[13] E. Feenberg, *Theory of Quantum Fluids* (Academic, New York, 1969).
[14] P. A. Whitlock, D. M. Ceperley, G. V. Chester, and M. H. Kalos, Phys. Rev. B **19**, 5598 (1979).
[15] M. H. Kalos, M. A. Lee, P. A. Whitlock and G. V. Chester, Phys. Rev. B **24**, 115 (1981).
[16] T. Morita, Prog. Theor. Phys. **20**, 920 (1958).
[17] J. M. J. van Leeuwen, J. Groenefeld, and J. de Boer, Physica **25**, 792 (1959).
[18] V. R. Pandharipande and R. B. Wiringa, Rev. Mod. Phys. **51**, 821 (1979).
[19] A. D. Jackson, A. Lande, and R. A. Smith, Phys. Rep. **86**, 55 (1982).
[20] A. D. Jackson, A. Lande, R. W. Guitink, and R. A. Smith, Phys. Rev. B **31**, 403 (1985).
[21] A. D. Jackson and T. Wettig, Phys. Rep. **237**, 325 (1994).

[22] A. D. Jackson, A. Lande, and R. A. Smith, Phys. Rev. Lett. **54**, 1469 (1985).
[23] S. Fantoni, Nuovo Cimento A **44**, 191 (1978).
[24] P. M. Lam and M. L. Ristig, Phys. Rev. B **20**, 1960 (1978).
[25] E. Manousakis, V. R. Pandharipande, and Q. N. Usmani, Phys. Rev. B **31**, 7022 (1985).
[26] E. Manousakis, V. R. Pandharipande, and Q. N. Usmani, Phys. Rev. B **43**, 13 587 (1991).
[27] C. E. Campbell, K. E. Kürten, M. L. Ristig, and G. Senger, Phys. Rev. B **30**, 3728 (1984).
[28] G. Senger, M. L. Ristig, K. E. Kürten, and C. E. Campbell, Phys. Rev. B **33**, 7562 (1986).
[29] G. Senger, M. L. Ristig, C. E. Campbell, and J. W. Clark, Ann. Phys. (N.Y.) **218**, 160 (1992).
[30] H.-W. He, Ph.D. thesis, Texas A&M University, 1992.
[31] D. M. Ceperley and E. L. Pollock, Phys. Rev. Lett. **56**, 351 (1986).
[32] B. H. Brandow, Ann. Phys. (N.Y.) **64**, 21 (1971).
[33] A. D. Jackson, A. Lande, and R. A. Smith, Phys. Rev. Lett. **54**, 1469 (1985).
[34] M. L. Ristig, in *From Nuclei to Particles*, Proceedings of the International School of Physics, Enrico Fermi, Course LXXIX, edited by A. Molinari (North-Holland, Amsterdam, 1981), p. 340.
[35] For the derivation, see T. Wettig, Ph.D. thesis, State University of New York at Stony Brook, 1994.
[36] J. C. Lee, Physica **93A**, 61 (1978).
[37] A. D. Jackson and R. A. Smith, Phys. Rev. A **36**, 2517 (1987).